J. Biochem. **144,** 323–333 (2008)
doi:10.1093/jb/mvn070

Important Amino Acid Residues that Confer CYP2C19 Selective Activity to CYP2C9

Yasunobu Wada[1], Maori Mitsuda[1], Yasuhiro Ishihara[2], Masatomo Watanabe[3], Masahiko Iwasaki[1,*] and Satoru Asahi[4]

[1]Department of Biology, Graduate School of Science, Osaka University, Osaka; [2]Laboratory of Pharmacology; [3]Laboratory of Molecular Pharmacology, Faculty of Pharmaceutical Sciences at Kagawa Campus, Tokushima Bunri University, Sanuki; and [4]Development Research Center, Pharmaceutical Research Division, Takeda Pharmaceutical Company Ltd, Osaka, Japan

Received April 18, 2008; accepted May 19, 2008; published online May 28, 2008

Although CYP2C9 and CYP2C19 display 91% sequence identity at the amino acid level, the two enzymes have distinct substrate specificities for compounds such as diclofenac, progesterone and (*S*)-mephenytoin. Amino acid substitutions in CYP2C9 were made based on an alignment of CYP2C9, CYP2C19 and monkey CYP2C43 sequences. Mutants of CYP2C9 were expressed in *Escherichia coli*. Sixteen amino acids, which are common to both CYP2C19 and CYP2C43 but different between CYP2C9 and CYP2C19, were substituted in CYP2C9 (CYP2C9-16aa). Next, the mutated amino acids in CYP2C9-16aa were individually reverted to those of CYP2C9 to examine the effect of each substitution on the enzymatic activity for CYP2C marker substrates. In addition, the role of the F–G loop in CYP2C9 and CYP2C19 was examined for substrate specificity and enzymatic activity. Our results showed: (i) CYP2C9-16aa displays 11% (*S*)-mephenytoin 4′-hydroxylase and full omeprazole 5-hydroxylase activity compared with that of CYP2C19; (ii) residue 286 is important for conferring CYP2C9-like enzyme activity on CYP2C9-16aa and residue 442 in CYP2C19 may be involved in the interaction with NADPH-P450 reductase; (iii) substitution of the F–G loop in CYP2C9 to that of CYP2C19 enhances tolbutamide *p*-methyhydroxylase and diclofenac 4′-hydroxylase activities and confers partial (*S*)-mephenytoin 4′-hydroxylase and omeprazole 5-hydroxylase activities, which are attributed to CYP2C19.

Key words: CYP2C9, CYP2C19, CYP2C43, F–G loop, NADPH-P450 reductase, substrate specificity.

Abbreviations: ABSF, 4-(2-aminoethyl)benzenesulfonyl fluoride·HCl; CYP, cytochrome P450; DTT, dithiothreitol; IPTG, isopropyl-β-D-thiogalactopyranoside; NADPH, nicotinamide adenine dinucleotide phosphate, reduced form; PCR, polymerase chain reaction.

Cytochromes P450 (CYP) comprise a superfamily of heme-containing enzymes. CYP1, 2 and 3 families in mammals have a wide range of overlapping substrate specificities and play a role in both drug and endogenous substrate metabolism (*1*). In humans, the CYP2C subfamily includes CYP2C8, 9, 18 and 19 (*2*). Among these isoforms, CYP2C9 and CYP2C19 share 91% amino acid identity, and there are 43 amino acid differences in a total of 490 residues. In spite of the high level of amino acid identity, diverse substrate specificities have been reported (*3*). CYP2C19 is responsible for 4′-hydroxylation of (*S*)-mephenytoin and is highly selective for proton pump inhibitors such as omeprazole 5-hydroxylation and lansoprazole 5-hydroxylation (*4*, *5*). However, structurally related CYP2C9 has little activity for these substrates, while both CYP2C9 and CYP2C19 catalyse tolbutamide *p*-methylhydroxylation in a similar manner (*5*, *6*). Ibeanu *et al*. (*7*) showed that residues 99, 220 and 221 of CYP2C19 are key determinants of omeprazole 5-hydroxylase activity from the results of chimeric constructs and amino acid substitutions between CYP2C9 and CYP2C19. However, analysis of these mutants clearly showed that changes in omeprazole 5-hydroxylase activity did not necessarily mirror those of (*S*)-mephenytoin 4′-hydroxylase activity. Thus the amino acid residues that determine substrate specificity for (*S*)-mephenytoin 4′-hydroxylation are distinct from those that confer omepraloze 5-hydroxylation activity. Recently, Matsunaga *et al.* (*8*) cloned CYP2C43 from monkey and showed it to exhibit (*S*)-mephenytoin 4′-hydroxylase activity. Furthermore, Mitsuda *et al.* (*9*) reported that CYP2C43 also posesses high progesterone 21-hyroxylase and testosterone 17-oxidase activity. Therefore, CYP2C43 is thought to be orthologous to CYP2C19 based on the amino acid sequence homology and substrate specificity. We reasoned that critical amino acid residues that determine substrate specificity may be identified by comparison of these CYP sequences. The F–G loop region forms part of the substrate access channel in CYP2C9 and CYP2C19 (*10*). This region of the enzyme, which was not altered to generate CYP2C9-16aa, was mutually

*To whom correspondence should be addressed. Tel: +81-(6)-6300-6697, Fax: +81-(6)-6300-6918,
E-mail: iwasaki_masahiko@takeda.co.jp

exchanged to examine the effect of amino acid substitutions.

In this study, we focused on the amino acid differences based on an alignment of CYP2C9, CYP2C19 and CYP43 sequences. From this analysis, 16 residues were chosen as candidate amino acids that may determine substrate specificity. We also substituted the F–G loop between CYP2C9 and CYP2C19 to evaluate the effect on substrate specificity and enzymatic activity. Amino acids of CYP2C9 were changed by site-directed mutagenesis and the mutated enzymes were expressed in *Escherichia coli* and purified. The effect of amino acid substitution was studied by comparing the activities for CYP2C marker substrates in a reconstitution system.

MATERIALS AND METHODS

Chemicals—(*S*)-Mephenytoin, 4′-hydroxymephenytoin, tolbutamide, hydroxytolbutamide, diclofenac sodium salt, 4′-hydroxydiclofenac and omeprazole were purchased from Daiichi Chemical Co. Ltd (Tokyo, Japan). Purified cytochrome b_5 was obtained from Pan Vera Corp. (Madison, WI). Microsomes (Supersomes^{TM}) from baculovirus-infected insect cells expressing human CYP2C19 or CYP2C9 with co-expressed human P450 reductase and human cytochrome b_5 were purchased from BD Biosciences (Woburn, MA). QAE-TOYOPEARL 650M and SP-TOYOPEARL 550C were obtained from TOSOH (Tokyo, Japan). Hydroxyapatite was purchased from Bio-Rad (Hercules, CA). Inertsil ODS-3 (150 mm × 4.6 mm I.D.) was obtained from GL Sciences Inc. (Tokyo, Japan). δ-Aminolevulinic acid was obtained from COSMO BIO (Tokyo, Japan). QuickChange Multi Site-Directed Mutagenesis Kit was purchased from Stratagene (La Jolla, CA). pCW vector was a gift from Professor F. W. Dahlquist (University of Oregon, Eugene, OR). Other chemicals were of the highest purity available.

Construction of CYP2C9 and CYP2C19 Plasmids, and Site-directed Mutagenesis—Plasmids for expression of CYP2C9 and CYP2C19 cDNAs in *E. coli* were provided by Takeda Pharmaceutical Company Ltd. The N-terminal encoding region of the cDNAs were modified and inserted into pCW vector as described previously (*9*, *11*). Mutations were introduced into CYP2C9 and CYP2C19 using QuickChange Multi Site-Directed Mutagenesis Kit according to the manufacturer's instructions. Oligonucleotides used for mutagenesis are listed in Tables 1–3. Mutants CYP2C9-15aa-50I and CYP2C9-13aa-72K/73P/74I were obtained in the process of mutating CYP2C9 to make the CYP2C9-16aa construct. Mutation was confirmed by

Table 1. **Sequence of oligonucleotide primers used to mutate CYP2C9 DNA for constructing CYP2C9-16aa.**

Mutant	Nucleotide sequence
2C9-50V	5′- TAGGTATTAAGGAC[G]TCAGCAAATCCTTAACC –3′
2C9-72E/73R/74M	5′- GTATTTTGGCCTG[G]AAC[G]CAT[G]GTGGTGCTGCATGG –3′
2C9-99H	5′- GTTTTCTGGAAGAGGC[CA]TTTCCCACTGGCTGAAAG –3′
2C9-119R	5′- TCAGCAATGGAAAGA[G]ATGGAAGGAGATCC –3′
2C9-237L	5′- TCACAACAAATTACTTAAAAAC[C]TTGCTTTTATGAAAAGTTATAT –3′
2C9-261R	5′- AATGGACATGAACAACCCTC[G]GGACTTTATTGATTGCTTCC –3′
2C9-269I	5′- TTTATTGATTGCTTCCTGAT[C]AAAATGGAGAAGGAAAAGCAC –3′
2C9-279Q	5′- AAGGAAAAGCACAACCAAC[A]ATCTGAATTTACTATTGAAAG –3′
2C9-286N	5′- CTGAATTTACTATTGAAA[A]CTTGGAAAACACTGCAGTTG –3′
2C9-374V	5′- CATGCAGTGACCTGTGAC[G]TTAAATTCAGAAACTATC –3′
2C9-410R	5′- AGATGTTTGACCCTC[G]TCACTTTCTGGATGA –3′
2C9-423N	5′- GCAATTTTAAGAAAAGTAA[C]TACTTCATGCCTTTCTCAG –3′
2C9-442R	5′- AGAAGCCCTGGCC[C]GCATGGAGCTGTTTT –3′
2C9-466D	5′- TGGTTGACCCAAAG[G]ACCTTGACACCACTC –3′

The base(s) that was altered to introduce the indicated mutation is marked by open square. The codon is underlined.

Table 2. **Sequence of oligonucleotide primers used to mutate CYP2C9-16aa for reverting amino acids to those of CYP2C9.**

Mutant	Nucleotide sequence
2C9-99I	5′- GTTTTCTGGAAGAGGC[AT]TTTCCCACTGGCTGAAAG –3′
2C9-119K	5′- TCAGCAATGGAAAGA[A]ATGGAAGGAGATCC –3′
2C9-237V	5′- TCACAACAAATTACTTAAAAAC[G]TTGCTTTTATGAAAAGTTATAT –3′
2C9-261R	5′- AATGGACATGAACAACCCTC[A]GGACTTTATTGATTGCTTCC –3′
2C9-269M	5′- TTTATTGATTGCTTCCTGAT[G]AAAATGGAGAAGGAAAAGCAC –3′
2C9-279P	5′- AAGGAAAAGCACAACCAAC[C]ATCTGAATTTACTATTGAAAG –3′
2C9-286S	5′- CTGAATTTACTATTGAAA[G]CTTGGAAAACACTGCAGTTG –3′
2C9-374I	5′- CATGCAGTGACCTGTGAC[A]TTAAATTCAGAAACTATC –3′
2C9-410H	5′- AGATGTTTGACCCTC[A]TCACTTTCTGGATGA –3′
2C9-423N	5′- GCAATTTTAAGAAAAGTAA[T]TACTTCATGCCTTTCTCAG –3′
2C9-442G	5′- AGAAGCCCTGGCC[G]GCATGGAGCTGTTTT –3′
2C9-466D	5′- TGGTTGACCCAAAG[A]ACCTTGACACCACTC –3′

The base(s) that was altered to introduce the indicated mutation is marked by open square. The codon is underlined.

Table 3. **Sequence of oligonucleotide primers used to mutate CYP2C9 and CYP2C19 in F–G loop.**

Mutant	Nucleotide sequence
CYP2C9-220P/221T	5′-CCAGATCTGCAATAATTTT□C□CA□CTATCATTGATTACTTCCC-3′
CYP2C19-220S/221P	5′-CCAGATCTGCAATAATTTT□T□C□TC□CTATCATTGATTACTTCCC-3′

The bases that were altered to introduce the indicated mutation are marked by open square. The codons are underlined.

sequencing using DNA sequencer SQ550 (Hitachi, Tokyo, Japan). Each plasmid with mutated cDNA was transformed into *E. coli* JM109.

Expression of CYP2C9, CYP2C19 and their Mutants in E. coli—CYP2C19, CYP2C9 and their mutants were expressed in *E. coli* as described previously (*11*). Transformed *E. coli* JM109 was grown overnight at 37°C in Luria–Bertani medium containing 50 μg/ml ampicillin. An 80 ml aliquot was inoculated into 8 l of modified Terrific Broth medium (12 g bactotyptone, 24 g yeast extract, 2 g bactopeptone, 50 mg thiamine and glycerol 4 ml/l) containing 50 μg/ml ampicillin and cultivated at 260 r.p.m. with an aeration rate of 0.5 v.v.m. [air volume (liquid volume)$^{-1}$ min^{-1}] at 30°C. δ-aminolevulinic acid (final conc. 0.5 mM) and isopropyl-β-D-thiogalactoside (IPTG) (final conc. 1 mM) were added when the absorbance of the culture broth (A_{600}) reached 0.2 and 0.3, respectively. The culture was continued for a further 24 h at 30°C before harvesting the cells by centrifugation at 10,000*g* for 20 min.

Preparation of Membrane Fractions from E. coli—All subsequent procedures were carried out at 4°C. Cells from the culture were resuspended in 100 mM Tris–HCl buffer (pH 7.4) containing 0.1 mM EDTA and 20% (v/v) glycerol. DNase I (2 units/ml) and lysozyme (0.3 mg/ml) were added to the cell suspension, and the mixture was gently stirred overnight and then centrifuged at 10,000*g* for 20 min. The pellet was resuspended (*ca* 0.5 g/ml) in 10 mM Tris–HCl buffer (pH 7.8) containing 0.1 mM 4-(2-aminoethyl)benzenesulfonyl fluoride·HCl (ABSF) and 20% (v/v) glycerol. The suspension was sonicated using an Astrason Ultrasonic Process XL (Heat Systems, Farmingdale, NY) at 50% of maximum output for 1 min with a 1 min interval between cycles. After 10 sonication cycles, the suspension was centrifuged at 10,000*g* for 20 min. The supernatant was further centrifuged at 100,000*g* for 60 min. The pellet (membrane fraction) was resuspended in 20% (v/v) glycerol using a homogenizer, and then stored at −80°C until use.

Purification of CYP2C9, CYP2C19 and their Mutants—The membrane fraction of *E. coli* expressing CYP2C9 was diluted to a final protein concentration of 2.0 mg/ml in 20 mM Tris–acetate buffer (pH 7.4) containing 20% (v/v) glycerol, 0.1 mM ABSF, 1 mM DTT, 1 mM EDTA, 0.6% (w/v) sodium cholate and 0.7% (w/v) Triton N-101 and stirred gently overnight in a total volume of 600 ml. After ultracentrifugation of the mixture at 100,000*g* for 60 min, the supernatant was applied to a QAE-TOYOPEARL 550C column (4.1 cm × 5 cm I.D.) equilibrated with 2 bed volumes of 20 mM Tris–HCl buffer (pH 7.4) containing 20% (v/v) glycerol, 0.1 mM ABSF, 1 mM dithiothreitol (DTT), 1 mM EDTA, 0.6% (w/v) sodium cholate and 0.7% (w/v) Triton N-101. The flow through fraction was collected and loaded directly onto a SP-TOYOPEARL 550C column (4.1 cm × 2.5 cm I.D.) equilibrated with 2 bed volumes of 10 mM potassium phosphate buffer (pH 6.5) containing 20% (v/v) glycerol, 0.5% (w/v) sodium cholate and 0.2% (w/v) Triton N-101. After washing with 2 bed volumes of 10 mM potassium phosphate buffer (pH 6.0) containing 20% (v/v) glycerol, 0.5% (w/v) sodium cholate and 0.5% (w/v) Triton N-101, CYP2C9 was eluted from the column with a linear gradient of 0–0.5 M NaCl in a total volume of 400 ml. Fractions containing CYP2C9 (as judged by SDS–polyacrylamide gel electrophoresis) were pooled and dialysed against 10 mM potassium phosphate buffer (pH 7.25) containing 20% (v/v) glycerol. The dialysed fraction was loaded onto a hydroxyapatite column (Type I, 2.5 cm × 2.5 cm I.D.) equilibrated with 5 mM potassium phosphate buffer (pH 7.25) containing 20% (v/v) glycerol, 0.5% (w/v) sodium cholate and 0.5% (w/v) Triton N-101. After washing the column with 2 bed volumes of 5 mM potassium phosphate buffer (pH 7.25) containing 20% (v/v) glycerol, 0.5% (w/v) sodium cholate and 0.5% (w/v) Triton N-101, CYP2C9 was eluted with a linear gradient of 5–500 mM potassium phosphate buffer (pH 7.25) in a total volume of 200 ml. The CYP2C9 fractions were pooled and dialysed against 5 mM potassium phosphate buffer containing 20% (v/v) glycerol. The dialysed fraction was loaded onto a hydroxyapatite chromatography column (Type I, 1 cm × 2.5 cm I.D.) equilibrated with 5 mM potassium phosphate buffer containing 20% (v/v) glycerol and 0.5% (w/v) sodium cholate. After washing the column with 10 bed volumes of 5 mM potassium phosphate buffer containing 20% (v/v) glycerol and 0.5% (w/v) sodium cholate, CYP2C9 was eluted with 500 mM potassium phosphate buffer (pH 7.25) containing 20% (v/v) glycerol and 0.7% (w/v) sodium cholate. The fractions containing CYP2C9 were pooled and dialysed against 30 mM phosphate buffer (pH 7.25) containing 20% (v/v) glycerol and 0.2% (w/v) sodium cholate. The procedure for purification of CYP2C19 and the mutants was the same as for CYP2C9.

Purification of NADPH-cytochrome P450—NADPH-cytochrome P450 was purified according to the method described by Yasukochi and Masters (*12*) from phenobarbital-treated rat liver microsomes. One unit of activity was defined as 1 μmol of cytochrome *c* reduced per minute. The specific activity of purified NADPH-cytochrome P450 reductase was 30 units/mg protein.

Protein Concentration Measurement—Protein concentration was measured using BCA Protein Assay Kit (Pierce Biotech., Rockford, IL) with bovine serum albumin as the protein standard.

Detection of CYP2C9, CYP2C19 and their Mutants—Cytochrome P450 content was measured from Fe^{+2}-CO versus Fe^{2+} difference spectrum according to the method described by Omura and Sato (*13*). Purity of P450 protein was checked by SDS–polyacrylamide gel electrophoresis using a 7.5–15% gradient gel. After electrophoresis proteins were stained with Bio-Safe CBB G-250 (Bio-Rad).

HPLC and MS Analysis of Omeprazole Metabolite—A mixture of Supersomes including 20 pmol CYP2C19 or CYP2C9 with 5 mM omeprazole was incubated in 20 mM HEPES buffer (pH 7.4) containing 0.1 mM EDTA and 1.5 mM $MgCl_2$ in the presence of 1 mM NADPH at 37°C for 30 min in a final volume of 200 µl. The reaction was stopped by adding 200 µl of acetonitrile and the mixture was centrifuged at 3,000 r.p.m. for 10 min. Omeprazole and its metabolites in the supernatant were analysed by LaChrom Elite HPLC system (HITACHI, Tokyo, Japan) (*14*). The HPLC conditions were as follows; column, Inertsil ODS-3 (150 mm × 4.6 mm I.D.) (GL Science Inc., Tokyo, Japan); mobile phase, methanol:actonitrile:H_2O (40:8:52); flow rate, 1.5 ml/min; and UV detection at 304 nm.

Omeprazole and its metabolites in the supernatant were further analysed by MALDI-TOF spectroscopy. The supernatant was dried by using a SpeedVac concentrator 2010 (Thermo Electron, Waltham, MA), and then resuspended in 0.1% trifluoroacetic acid (TFA) and loaded into a µ-C18 ZipTip (Millipore). The bound omeprazole and its metabolites were eluted from the ZipTip with 0.5 µl of α-cyano-4-hydroxycinnamic acid (α-CHCA). The α-CHCA matrix concentration was 10 mg/ml in a mixture of acetonitrile:water containing 0.1% TFA (40:60 v/v). Each sample was analysed by an AXIMA-CFR plus (Shimadzu Biotech, Kyoto, Japan) mass spectrometer. All spectra were acquired in the positive linear mode. Mass calibration was performed using internal two α-CHCA ion species, $[M+H]^+$ at *m/z* 190.0504 and $[2M+H]^+$ at *m/z* 379.0930.

Enzyme Assays—A typical reaction mixture consisted of 50 pmol cytochrome P450, 100 pmol cytochrome b_5, 0.5 units of NADPH-P450 reductase, 20 µg of dilauroylphosphatidylcholine, 50 mM HEPES buffer (pH 7.4), 0.1 mM EDTA, 1.5 mM $MgCl_2$ and the substrate in a final volume of 200 µl. After pre-incubation at 37°C for 5 min, the reaction was started by the addition of 20 µl of 10 mM NADPH, and continued for 30 or 60 min depending on the substrate (see later) with gentle stirring at 37°C. Substrate concentrations were as follows: (*S*)-mephenytoin, 500 µM; tolbutamide, 500 µM; diclofenac, 100 µM and omeprazole, 500 µM. All assays were conducted in triplicate except that omeprazole 5-hydroxylation to compare the activity of CYP2C9-16aa and its mutants were measured in duplicate.

(*S*)-Mephenytoin 4′-hydroxylation was determined by the procedure described by Romkes *et al*. (*2*) with minor modifications. After incubation for 30 min at 37°C, 200 µl of acetonitrile was added to stop the reaction, and the mixture centrifuged at 3,000 r.p.m. for 10 min. A 50 µl aliquot of sample was analysed by HPLC. The HPLC conditions were as follows: column, Inertsil ODS-3 (150 mm × 4.6 mm I.D.) (GL Sciences Inc., Tokyo, Japan); mobile phase, acetonitrile:10 mM phosphate buffer (pH 7.4) (26:74, v/v); flow rate, 1.0 ml/min; column oven temperature, 40°C and UV detection at 224 nm.

Tolbutamide *p*-methylhydroxylation was determined by the procedure described by Richardson *et al*. (*11*) with modifications. After incubation for 60 min, the reaction was terminated by the addition of 200 µl of acetonitrile and centrifuged at 3,000 r.p.m. for 10 min. An aliquot was analysed by HPLC. The HPLC conditions were as follows: column, Inertsil ODS-3 (150 mm × 4.6 mm I.D.) (GL Science Inc., Tokyo, Japan); mobile phase, acetonitrile:H_2O:acetic acid (100:900:1) (solvent A) and acetonitrile:H_2O:perchlorid acid (900:100:1) (solvent B); time program of solvent B, 0% (1–6 min), 0–50% (6–9 min), 50% (9–16 min), 50–0% (16–16.1 min), 0% (16.1–26 min) and UV detection at 230 nm.

Diclofenac 4′-hydroxylation was measured by the procedure described by Tang *et al*. (*15*) with minor modifications. The reaction was continued for 30 min at 37°C, and terminated by the addition of 200 µl of acetonitrile, and followed by the centrifugation at 3,000 r.p.m. for 10 min. An aliquot was analysed by HPLC. The HPLC conditions were as follows: column, Inertsil ODS-3 (150 mm × 4.6 mm I.D.) (GL Science Inc., Tokyo, Japan); mobile phase, acetonitrile:H_2O:acetic acid (100:900:1) (solvent A) and acetonitrile:H_2O:acetic acid (900:100:1) (solvent B); a flow rate, 1.0 ml/min; time program of solvent B, 50% (0–8 min), 50–90% (8–18 min), 90–50% (18–18.1 min), 50% (18.1–25 min) and UV detection at 280 nm.

Omeprazole 5-hydroxylation in reconstitution was determined as described in '*HPLC and MS analysis of omeprazole metabolite*'. Formation of the metabolite was calculated based on the assumption that the molecular extinction coefficient of 5-hydroxy omeprazole was the same as that for omeprazole.

RESULTS

Selection of Amino Acids for Site-directed Mutagenesis—An amino acid sequence alignment of CYP2C9, CYP2C19 and CYP2C43 is shown in Fig. 1. CY2C43 displays 95 and 94% amino acid identity with CYP2C9 and CP2C19, respectively. CYP2C43 cloned from monkey liver was considered to be orthologous to CYP2C19 in terms of (*S*)-mephenytoin 4′-hydroxylase, progesterone 21-hydroxylase and testosterone 17-oxidase activity (*8*, *9*). Thus, we assumed that CYP2C19 and CYP2C43 share the same amino acids for (*S*)-mephenytoin 4′-hydroxylase activity. A total of 16 residues that are likely to be involved in substrate recognition were chosen based on the amino acid sequence comparison among CYP2C9, CYP2C19 and CYP2C43. The candidate residues can be divided into two groups: First, amino acid residues in CYP2C19 that are the same as those in CYP2C43 but different from CYP2C9. These include 15 amino acid residues at positions 50, 72, 73, 74, 99, 119, 261, 269, 279, 286, 374, 410, 423, 442 and 466. Secondly, amino acid residue 237 is different in CYP2C9, CYP2C19 and CYP2C43. These 16 amino acids are highlighted in Fig. 1.

Substitution of Amino Acids of CYP2C9 and CYP2C19—The aforementioned 16 amino acids in CYP2C9 were substituted to those of CYP2C19 at I50V, K72E, P73R, I74M, I99H, K119R, V237L, Q261R, M269I, P279Q, S286N, I374V, H410R, K423N, G442R and D466N. Among these amino acids, residues 99, 237 and 286 fall into the substrate recognition site (SRS) 1, 3 and 4, respectively (*16*). We refer to the 16 amino-acid-substituted CYP2C9 as CYP2C9-16aa. Furthermore, residues in CYP2C9-16aa were reverted to those of CYP2C9 either by a single amino acid substitution or as

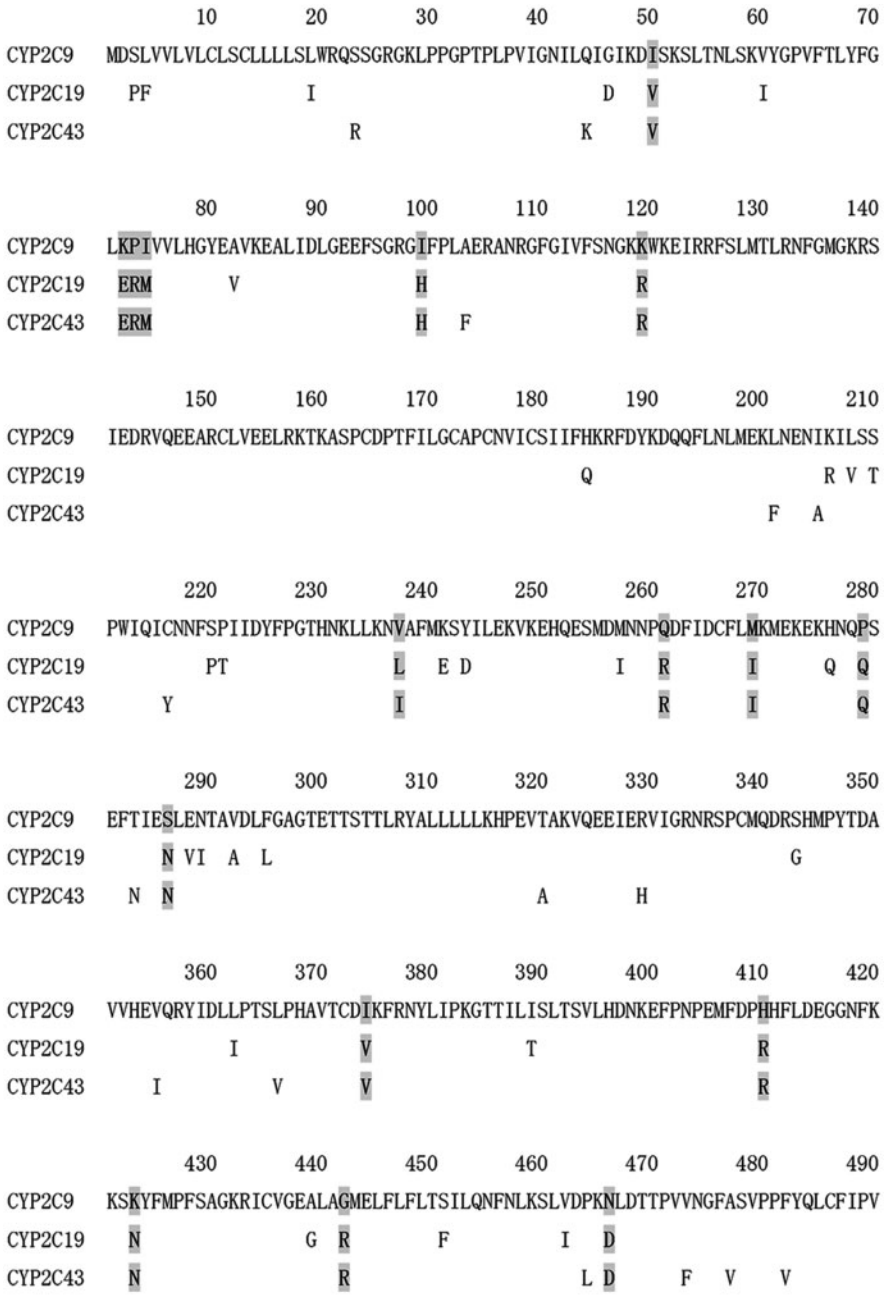

Fig. 1. **Alignment of human CYP2C9, CYP2C19 and monkey CYP2C43 amino acid sequences.** For clarity, only these different amino acid residues were shown in the above alignment. Shadowed amino acid residues, which are found in both CYP2C19 and CYP2C43 but different between CYP2C9 and CYP2C19, were chosen for the site-directed mutagenesis.

a three amino acid unit en bloc (*i.e.* residues 72, 73 and 74). These mutants included CYP2C9-15aa-50I, CYP2C9-13aa-72K/73P/74I, CYP2C9-15aa-99I, CYP2C9-15aa-119K, CYP2C9-15aa-237V, CYP2C9-15aa-261Q, CYP2C9-15aa-279P CYP2C9-P15aa-286S, CYP2C9-15aa-374I, CYP2C9-15aa-410H, CYP2C9-15aa-423K, CYP2C9-15aa-442G and CYP2C9-15aa-466D. For example, CYP2C9-15aa-50I denotes amino acid at 50 in CYP2C9-16aa was changed from V to I.

Reciprocal substitutions in the F–G loop between CYP2C9 and CYP2C19 were introduced by changing amino acid residues at 220 and 221 (Fig. 2). S220 and P221 in CYP2C9, P220 and T221 in CYP2C19, were changed to 220P and 221T (CYP2C9-220P/221T), 220S and 221P (CYP2C19-220S/221P), respectively.

Purification of CYP2C9, CYP2C19 and their Mutants—CYP2C9, CYP2C19 and their mutants were expressed in *E. coli* and the membrane fractions were prepared. After solubilization of the membrane, CYPs were purified by sequential column chromatography steps. The CO-reduced difference spectra of the purified CYPs showed a peak at 450 nm without conversion to P420 (data not shown) and the specific contents of the purified CYPs were higher than 9.79 nmol P450/mg protein (Table 4).

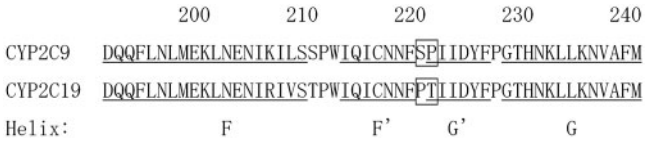

Fig. 2. **Alignment of CYP2C9 and CYP2C19 amino acid sequences surrounding the F–G loop.** Amino acids in open squares were mutated reciprocally between CYP2C9 and CYP2C19.

Table 4. **Purified CYP2C9, CYP2C19 and their mutants from *E. coli* membrane fraction.**

	Protein (mg/ml)	P450 (nmol/ml)	Specific content (nmol/mg)
CYP2C9	1.35	16.3	12.1
CYP2C19	3.43	34.3	9.97
CYP2C-16aa	1.59	21.1	13.3
CYP2C-16aa mutant			
15aa-50I	2.64	43.1	14.9
13aa-72K/73P/74I	2.30	36.6	16.3
15aa-99I	2.00	24.6	12.3
15aa-119K	2.45	40.4	16.5
15aa-237V	2.11	29.9	14.2
15aa-261Q	2.61	36.3	16.9
15aa-279P	2.03	34.3	16.9
15aa-286S	2.76	40.4	14.7
15aa-374I	1.34	16.7	12.5
15aa-410H	1.42	23.7	16.7
15aa-423K	1.30	18.0	13.8
15aa-442G	1.93	21.5	14.5
15aa-466D	2.03	29.9	14.7
CYP2C9-220P/221T	3.11	44.8	14.2
CYP2C19-220S/221P	2.30	36.0	15.7

Analysis of Omeprazole Metabolite—Omeprazole showed a single peak at 11.5 min (Fig. 3A). A single omeprazole metabolite was detected with the incubation of Supersomes expressing CYP2C19 at 4.7 min (Fig. 3B), while metabolite was not observed with the incubation of Supersomes expressing CYP2C9 (Fig. 3C). The HPLC profile of the omeprazole metabolite was similar to that of metabolite formed by yeast microsomes expressing CYP2C19 (*17*). MS analysis was carried out to analyse the omeprazole metabolite. The monoisotopic peak of omeprazole was observed at *m/z* 298.1 (Fig. 3E and F), while the omeprazole metabolite formed by the incubation with Supersomes expressing CYP2C19 showed the peak at *m/z* 314.1 (Fig. 3G). The molecular weight of the metabolite was shown to be 16 higher than that of omeprazole. Thus, the omeprazole metabolite was confirmed as 5-hydroxy omeprazole previously reported by Hofmann *et al*. (*18*).

Metabolic Activities of CYP2C9-16aa and its Mutants Towards CYP2C Marker Substrates—(*S*)-Mephenytoin 4′-Hydroxylation

(*S*)-Mephenytoin 4′-hydroxylation is regarded as a marker activity for CYP2C19 (*7*). Figure 4A shows a comparison of (*S*)-mephenytoin 4′-hydroxylase activity among CYP2C9, CYP2C19, CYP2C9-16aa and a series of mutants derived from CYP2C9-16aa. CYP2C19 exhibited (*S*)-mephenytoin 4′-hydroxylase activity (2.54 nmol/min/nmol P450), whereas CYP2C9 was not active toward this substrate confirming the previous reports by Ibeanu *et al*. (*7*). However, CYP2C9-16aa showed low but significant (*S*)-mephenytoin 4′-hydroxylase activity (0.27 nmol/min/nmol P450), which was 11 and 36% that of CYP2C19 and CYP2C43 (0.75 nmol/min/nmol P450, unpublished observation by Wada *et al*.), respectively. Among CYP2C9-16aa mutants, CYP2C9-15aa-99I, CYP2C-15aa-286S and CYP2C9-15aa-442G exhibited relatively low (*S*)-mephenytoin 4′-hydroxylase activity with the metabolic rate of 0.11, 0.12 and 0.06 nmol/min/nmol P450, corresponding to 41, 44 and 22% that of CYP2C9-16aa, respectively.

Tolbutamide *p*-methylhydroxylation

Tolbutamide *p*-methylhydroxylase activity has been reported to be attributed both to CYP2C9 and CYP2C19 (*19*). Figure 4B shows tolbutamide *p*-methylhydroxylase activity of CYP2C9, CYP2C19, CYP2C9-16aa and a series of mutants derived from CYP2C9-16aa. CYP2C9 and CYP2C19 exhibited similar tolbutamide *p*-methylhydroxylase activity with a metabolic rate of 2.5 and 1.98 nmol/min/nmol P450, respectively. Tolbutamide *p*-methylhydroxylase activity of CYP2C9-16aa (3.46 nmol/min/nmol P450) was 1.4-fold that of CYP2C9. However, CYP2C9-15-aa-237V, CYP2C9-15aa-286S and CYP2C9-15aa-423K showed tolbutamide *p*-methylhydroxylase activity of 7.71, 7.03 and 4.93 nmol/min/nmol P450, which is 2.2-, 2.0- and 1.4-fold higher than that of CYP2C9-16aa, respectively. However, tolbutamide *p*-methylhydroxylase activity of CYP2C9-15aa-442G (0.39 nmol/min/nmol P450) was significantly reduced to 11% that of CYP2C9-16aa.

Diclofenac 4′-hydroxylation

Diclofenac 4′-hydroxylation is catalysed primarily by CYP2C9 (*19*). Figure 4C shows diclofenac 4′-hydroxylase activity of CYP2C9, CYP2C19, CYP2C9-16aa and a series of mutants derived from CYP2C9-16aa. CYP2C9 and CYP2C19 exhibited diclofenac 4′-hydroxylase activity at a rate of 15.9 and 1.1 nmol/min/nmol P450, respectively. CYP2C9-16aa catalysed diclofenac 4′-hydroxylation at a rate of 21.9 nmol/min/nmol P450, which is 1.4-fold that of CYP2C9. CYP2C9-15aa-286S and CYP2C9-15aa-423K showed diclofenac 4′-hydroxylase activity at a rate of 34.5 and 30.5 nmol/min/nmol P450 (*i.e*. 1.6- and 1.4-fold higher than that of CYP2C9-16aa, respectively). However, diclofenac 4′-hydroxylase activity of CYP2C9 15aa-442G (6.95 nmol/min/nmol P450) was reduced to 32% that of CYP2C9-16aa.

Omeprazole 5-hydroxylation

Omeprazole 5-hydroxylation is regarded as a marker activity for CYP2C19 (*7*). Figure 4D shows omeprazole 5-hydroxylase activity of CYP2C9, CYP2C19, CYP2C9-16aa and a series of mutants derived from CYP2C9-16aa. CYP2C9 did not display appreciable omeprazole 5-hydroxylase activity, while CYP2C19 showed omeprazole 5-hydroxylase activity at a rate of 3.85 nmol/min/nmol P450. However, CYP2C9-16aa exhibited omeprazole 5-hydroxylase activity at a rate of 4.58 nmol/min/nmol

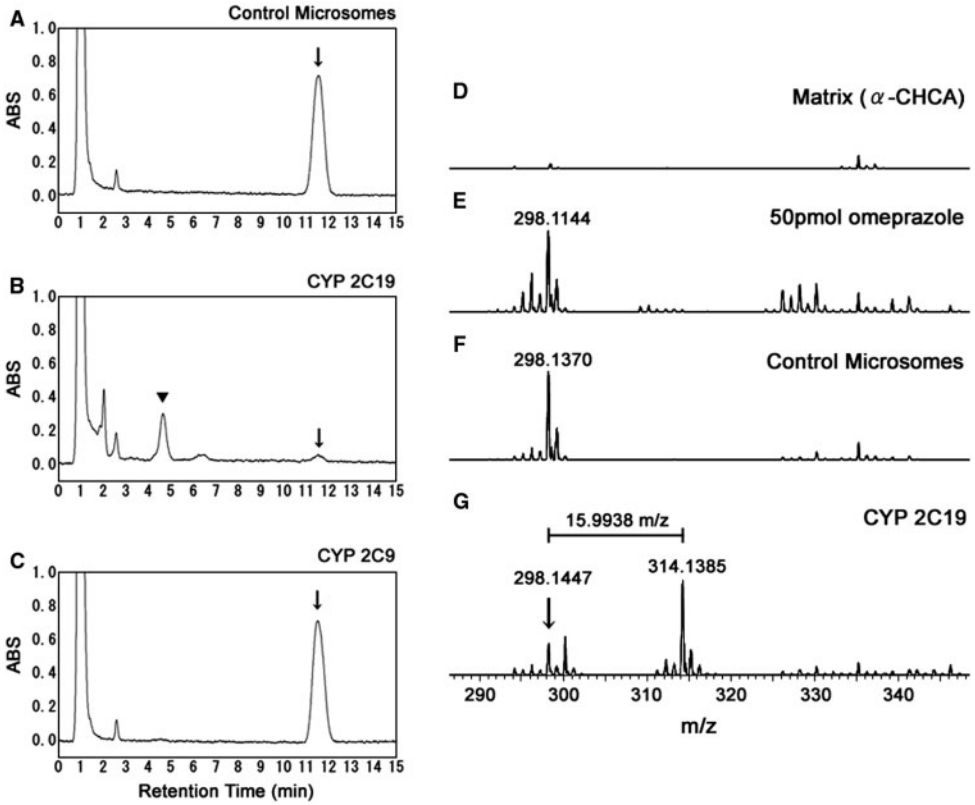

Fig. 3. **HPLC and MS analysis of omeprazole and its metabolites.** Supersomes were incubated with 5 μM omeprazole and analysed by HPLC using Intertsil ODS-3 (150 mm × 4.6 mm I.D.) (A–C). (A) Control microsomes. (B) Supersomes expressing CYP2C19. (C) Supersomes expressing CYP2C9. Arrow and triangle indicate omeprazole and its metabolite, respectively. Omeprazole and its metabolite were analysed by MALDI-TOF MS (D–G). (D) α-CHCA matrix without sample for comparison. (E) 50 pmol omeprazole. (F) Control microsomes. (G) Supersomes expressing CYP2C19.

P450, which is similar to that of CYP2C19. CYP2C9-15aa-286S, CYP2C9-15aa-410H and CYP2C9-15aa-442G exhibited omeprazole 5-hydroxylase activity at a rate of 2.61, 2.44 and 2.18 nmol/min/nmol P450, which is 57, 53 and 48% that of CYP2C19-16aa, respectively.

Effect of Reciprocal Substitution of F–G loop between CYP2C9 and CYP2C19 on Metabolic Activities—The F–G loop, which does not include any of the 16 amino acid substitutions made to generate CYP2C9-16aa, was reciprocally changed between CYP2C9 and CYP2C19 to examine the effect on enzyme activity and substrate specificity (Fig. 2). CYP2C9 did not show detectable activity for (*S*)-mephenytoin 4′-hydroxylation and omeprazole 5-hydroxylation. However, CYP2C9-220P/221T displayed both (*S*)-mephenytoin 4′-hydroxylase (0.07 nmol/min/nmol P450) and omeprazole 5-hydroxylase activity (1.91 nmol/min/nmol P450), which were 3% (2.46 nmol/min/nmol P450) and 44% (4.30 nmol/min/nmol P450) that of CYP2C19, respectively (Fig. 5A and D). Interestingly, tolbutamide *p*-methylhydroxylase activity of CYP2C9 (2.20 nmol/min/nmol P450) was increased 2.6-fold in CYP2C9-220P/221T (5.63 nmol/min/nmol P450) (Fig. 5B). Furthermore, diclofenac 4′-hydroxylase activity of CYP2C9-220P/221T (46.7 nmol/min/nmol P450) was similarly enhanced 3.0-fold compared with that of CYP2C9 (15.9 nmol/min/nmol P450) (Fig. 5C). Conversely, mutated CYP2C19-220S/221P showed similar (*S*)-mephenytoin 4′-hydroxylase, tolbutamide *p*-methylhydroxylase, diclofenac 4′-hydroxylase and omeprazole 5-hydroxylase activities to that of CYP2C19 (Fig. 5A–D).

DISCUSSION

CYP2C9 does not show appreciable omeprazole 5-hydroxylase and (*S*)-mephenytoin 4′-hydroxylase activity, however, these activities were conferred to CYP2C9-16aa (*i.e.* full activity and 11% that of CYP2C19, respectively). Thus, the amino acid substitutions used to generate CYP2C9-16aa did not appear to interfere with the molecular recognition of substrates of CYP2C9 used in this study. Our results are consistent with previous studies that have identified specific amino acids in CYP2C19, which are important for substrate specificity, including residue 99 located in the interhelical region of B and B′ helices (*7*, *10*) (Fig. 6).

CYP2C9-15aa-442G displayed reduced CYP2C19 marker activities [(*S*)-mephenytoin 4′-hydroxylase and omeprazole 5-hydroxylase], and CYP2C9 activities (tolbutamide *p*-methylhydroxylase and diclofenac 4′-hydroxylase). Amino acid 442 is located in the L helix on the proximal surface opposite the substrate binding site

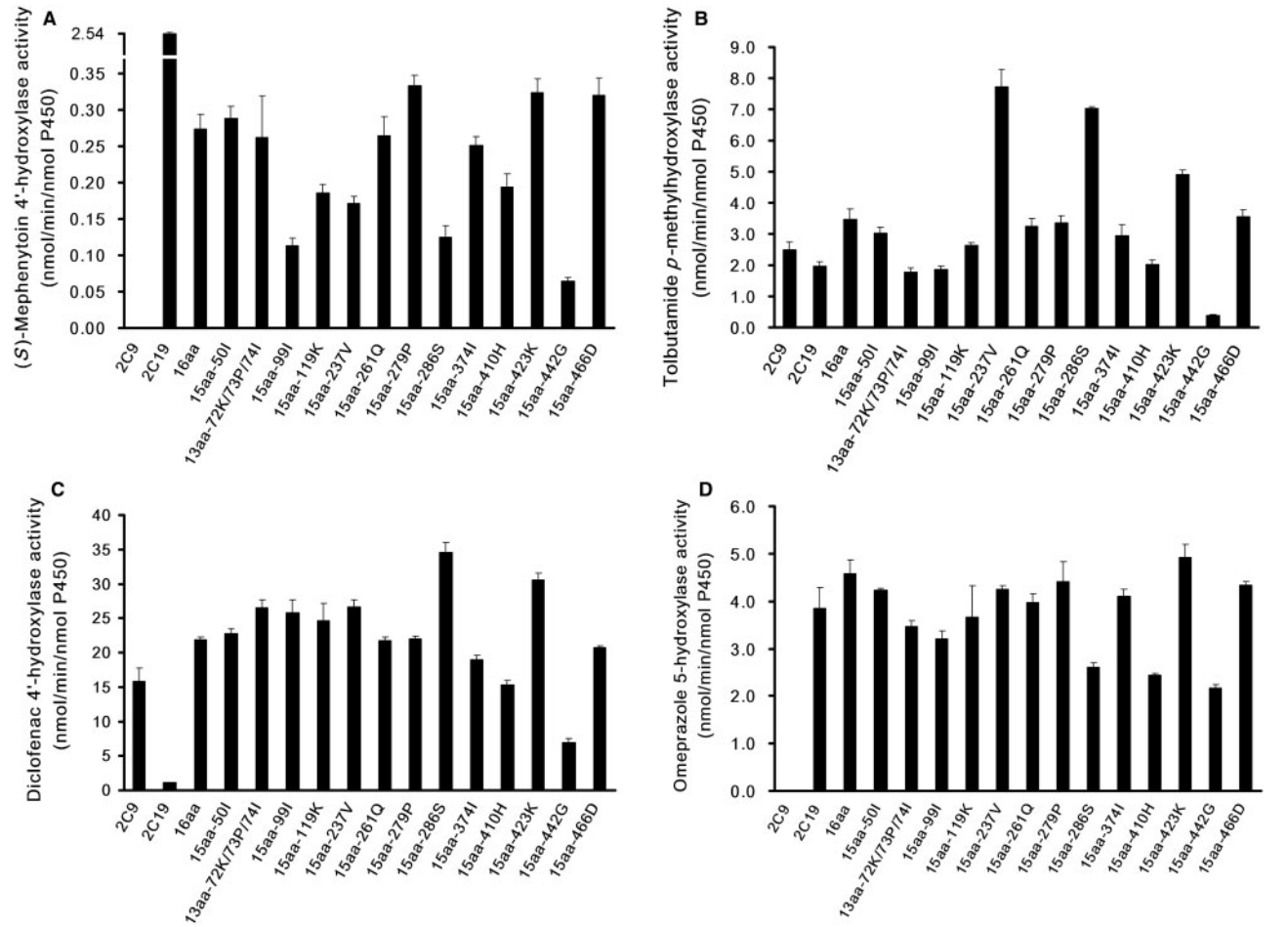

Fig. 4. **Metabolic activities exhibited by CYP2C9, CYP2C19, CYP2C9-16aa and a series of CYP2C9-16aa mutants in reconstitution.** (A) (*S*)-Mephenytoin 4′-hydroxylase activity. (B) Tolbutamide *p*-methylhydroxylase activity. (C) Diclofenac 4′-hydroxylase activity. (D) Omeprazole 5-hydroxylase activity. Data are the means ± SD of three determinations (A–C) or the means ± error of two determinations (D).

across the heme group (*20*, *21*) (Fig. 6). The amino acid corresponding to 442 in human CYP2C subfamily as well as monkey CYP2C20 and CYP2C43 is conserved as Arg except for Gly in CYP2C9 (*9*, *22*, *23*). The proximal surface of P450 has a strong positive electrostatic potential in the region of helix C and near the heme group and is implicated in the interaction with NADPH-P450 reductase. In CYP2B4, the amino acid, which corresponds to 442 in CYP2C9, is Arg at residue 443. The amino acid change at 443 from Arg to Ala exhibited decreased binding to NADPH-P450 reductase, leading to reduced metabolic activity (*24*). A novel single nucleotide polymorphism of CYP2C19 was found in which amino acid Arg was substituted to Cys at residue 442 (*25*). This substitution reduced the *in vivo* capacity for mephobarbital 4′-hydroxylation, which is catalysed by CYP2C19. Therefore, residue 442 appears to be involved in the transfer of electron, rather than exerting an effect on substrate specificity.

CYP2C9-15aa-237V and CYP2C9-15aa-286S displayed lower activity for CYP2C19 marker substrates [(*S*)-mephenytoin and omeprazole], but increased activity for CYP2C9 marker substrates (tolbutamide and diclofenac). These results underscore the reciprocal effect of amino acid 237 and 286 on the metabolic activity for CYP2C9 and CYP2C19 substrates. The important role of amino acids 237 and 286, which are in I and L helices (Fig. 6) and fall on SRS3 and 4, respectively, was reported for (*S*)-mephenytoin 4′-hydroxylation, amino pyrine *N*-demethylation and testosterone 17-oxidation from the chimeras between CYP2C9 and CYP2C19 (*26*). Enhanced tolbutamide *p*-methylhydroxylase and diclofenac 4′-hydroxylase activity of CYP2C9-15aa-286S was consistent with the chimera 19/Sma-Eco 9 (residues 228–282 of CYP2C9) containing amino acid residues at N288E and I289N of CYP2C9 in SRS4. The chimera increased tolbutamide *p*-methylhydroxylase, diclofenac 4′-hydroxylase and ibuprofen hydroxylase activity by the introduction of mutation N286S, an amino acid change from CYP2C19 to CYP2C9 (*19*). Jung *et al*. also reported that the KSN mutant of CYP2C19 (2C19: E241K, N286S and I289N) exhibited the capacity of CYP2C19 to metabolize both (R)- and (S)-warfarin with a broad regioselectivity (*27*).

CYP2C9-15aa-99I reduced (*S*)-mephenytoin 4′-hydroxylase activity, while omeprazole 5-hydroxylase activity

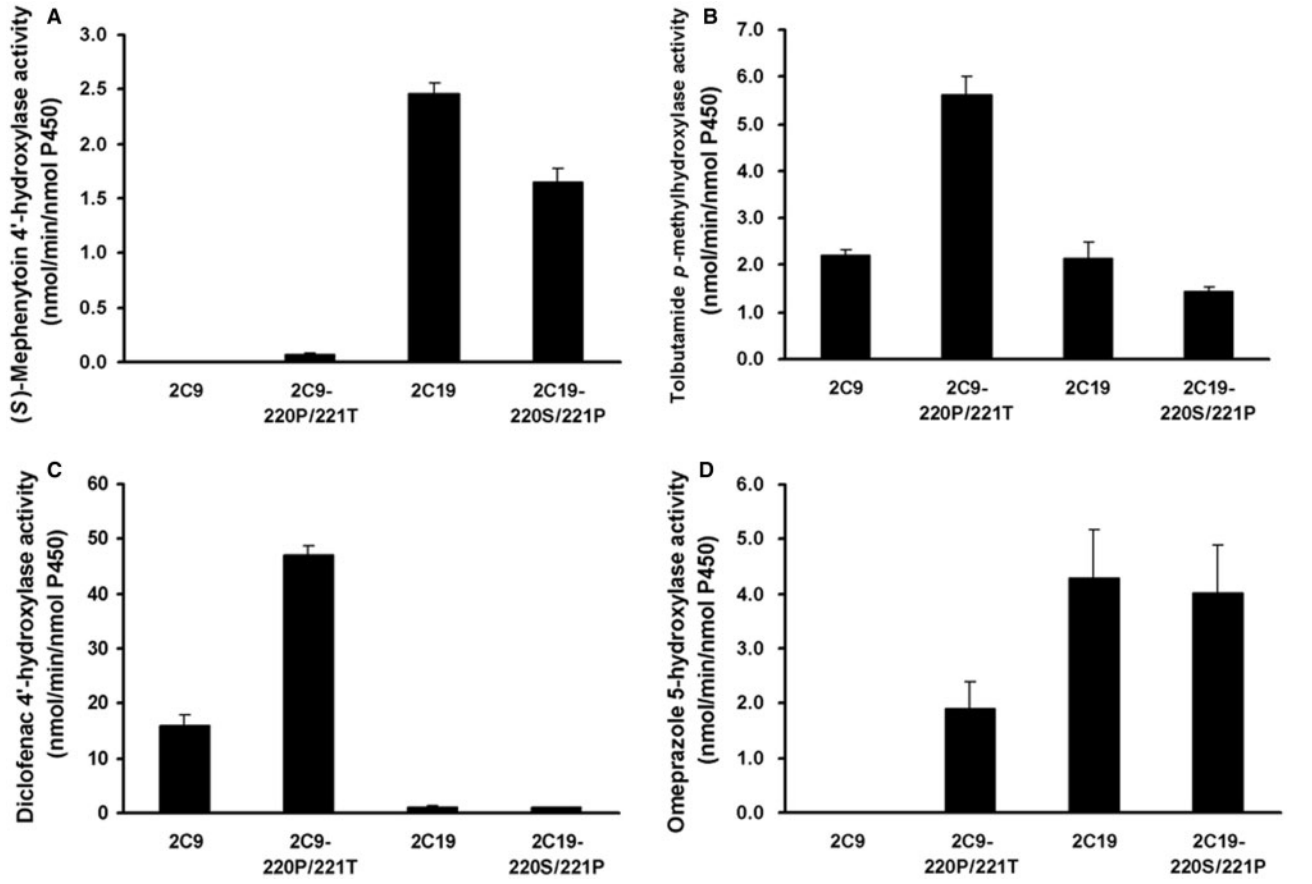

Fig. 5. **Metabolic activities exhibited by CYP2C9, CYP2C9-220P/221T, CYP2C19 and CYP2C19-220S/221P in reconstitution.** (A) (*S*)-Mephenytoin 4′-hydroxylase activity. (B) Tolbutamide *p*-methylhydroxylase activity. (C) Diclofenac 4′-hydroxylase activity. (D) Omeprazole 5-hydroxylase activity. Data are the means ± SD of three determinations.

was almost unaffected. CYP2C9-15aa-410H reduced omeprazole 5′-hydroxylase activity, whereas (*S*)-mephenytoin 4′-hydroxylase activity was almost unchanged. Therefore, contributions of these amino acids seem to differ in the CYP2C19 marker activity depending on the substrate, such as (*S*)-mephenytoin and omeprazole. CYP2C9-15aa-423K increased metabolic activity only for CYP2C9 marker substrates (tolbutamide and diclofenac). Thus, amino acid 423 might be located in a position to distinguish between CYP2C9 and CYP2C19 substrates. Amino acids 410 and 423 are located in the 'meandering region' (*28*, *29*) (Fig. 6). In particular, amino acid 410 lies in the center of the consensus sequence of Pro X Arg/His (*30*). It is speculated that these amino acids in the 'meandering region', which is outside of SRSs forming a protruding loop on the surface of the P450 enzymes, are also involved in changing catalytic activities as seen in the studies with CYP4B1 and CYP1A2 (*31*, *32*).

According to molecular structural analysis, the F–G loop is considered to form a flexible lid and a substrate entrance channel in CYP2C8, CYP2C9 and CYP2B4 (*33*–*35*). Substitution of the F–G loop in CYP2C19 to that of CYP2C9 (CYP2C19–220S/221P) did not affect the metabolic activities of CYP2C9 marker substrates. However, substitution of the F–G loop in CYP2C9 to that of CYP2C19 (CYP2C9–220P/221T) not only

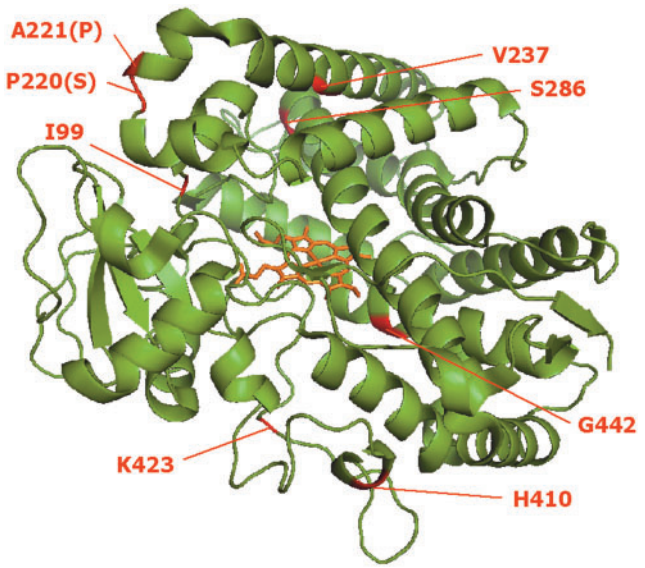

Fig. 6. **Amino acid residues in CYP2C9 to confer enzyme selectivity found in this study.** Amino acid positions, 99, 220, 221, 237, 286, 410 and 442, are indicated in the 3D model of CYP2C9 in which S220P and P221A mutations were introduced (*20*).

showed an increase in tolbutamide *p*-methylhydroxylase and diclofenac 4′-hydroxylase activities, but also conferred (*S*)-mephenytoin 4′-hydroxylase and omeprazole 5-hydroxylase activities which were not detectable in CYP2C9. These results highlight the critical role of amino acids 220 and 221 of CYP2C9–220P/221T in the metabolism of substrates for both CYP2C9 and CYP2C19 marker substrates. Ibeanu *et al.* (*7*) reported that a single amino acid substitution at I99H conferred about 50% omeprazole hydroxylase activity to CYP2C9 and additional mutations at 220 and 221 to those of CYP2C19 gave almost full activity, whereas a single I99H and I99H/S220P/P221S substitutions in CYP2C9 did not result in (*S*)-mephenytoin hydroxylase activity. However, our data shows that residues 220 and 221 are also important for conferring (*S*)-mephenytoin 4′-hydroxylase and omeprazole 5-hydroxylase activity and that the I99H substitution is not necessarily a prerequisite for changing the substrate specificity. Recently, two crystal structures of CY2C9 have been published (*21*, *34*). The CYP2C9 structure bound with warfarin showed that the F′–G′ region (Fig. 2), which was replaced with that of CYP2C5, forms a helix (*20*) (Fig. 6). However, a separate study of the wild-type CYP2C9 structure showed that helix G′ was not evident and that the F–G loop exhibits an extended structure (*21*). The authors of the report speculated that the position of P220, as found in CYP2C8 and CYP2C5, might contribute to stabilizing the helix F′–G′ region, which was also reported in the warfarin-bound CYP2C9 structure. CYP2C9-220P/221T might assume a stable F′–G′ helix, as shown in the CYP2C8 and CYP2C5 crystal structures, to form a conduit for access and egress of small molecular weight compounds. Our results recapitulate the importance of the F–G loop in determining substrate specificity and activity within the cytochrome P450 2C subfamily.

In conclusion, we introduced mutations in CYP2C9 amounting to 16 amino acid residues that are considered important for substrate specificity based on an alignment of CYP2C9, CYP2C19 and CYP2C43 sequences. In addition, we substituted the F–G loop in CYP2C9 and CYP2C19. Our results showed that (i) the 16 amino acid-mutated mutant, CYP2C9-16aa, exhibits 11% (*S*)-mephenytoin 4′-hydroxylase and full omeprozole 5-hydroxylase activity compared with that of CYP2C19, while retaining catalytic activities of CYP2C9; (ii) residues 237 and 286 were also shown to be important in determining CYP2C9-like enzyme activity in CYP2C9-16aa, while amino acid residues 410 and 423 located out side of SRSs were involved in CYP2C19-like activity, and the charged amino acid 442 in CYP2C19 was implicated in the interaction with NADPH-P450 reductase; (iii) two amino acid substitutions at 220S and 221P in F–G loop of CYP2C9 to CYP2C19 were found to enhance tolbutamide *p*-methylhydroxylase and diclofenac 4′-hydroxylase activity and confer minimal (*S*)-mephenytoin 4′-hydroxylase and moderate omeprozole 5-hydroxylase activity to CYP2C9.

We would like to thank Dr Norio Shimamoto for helpful discussions. We are also grateful to Dr Sumie Yoshitomi and Ms Keiko Ikemoto for their technical guidance throughout this study and Dr Toshimasa Tanaka for drawing CYP2C9 3D structure. We thank Dr Kenji Okonogi and Dr Tetsuo Miwa for their encouragement throughout this study, and express our gratitude to Dr E. Dahlquist for providing the pCW expression vector.

REFERENCES

1. Anzenbacher, P. and Anzenbacherova, E. (2001) Cytochromes P450 and metabolism of xenobiotics. *Cell Mol. Life Sci.* **58**, 737–747
2. Romkes, M., Faletto, M.B., Blaisdell, J.A., Raucy, J.L., and Goldstein, J.A. (1991) Cloning and expression of complementary DNAs for multiple members of the human cytochrome P450IIC subfamily. *Biochemistry* **30**, 3247–3255
3. Goldstein, J.A. and de Morais, S.M. (1994) Biochemistry and molecular biology of the human CYP2C subfamily. *Pharmacogenetics* **4**, 285–299
4. Chiba, K., Kobayashi, K., Manabe, K., Tani, M., Kamataki, T., and Ishizaki, T. (1993) Oxidative metabolism of omeprazole in human liver microsomes: cosegregation with S-mephenytoin 4′-hydroxylation. *J. Pharmacol. Exp. Ther.* **266**, 52–59
5. Goldstein, J.A., Faletto, M.B., Romkes-Sparks, M., Sullivan, T., Kitareewan, S., Raucy, J.L., Lasker, J.M., and Ghanayem, B.I. (1994) Evidence that CYP2C19 is the major (S)-mephenytoin 4′-hydroxylase in humans. *Biochemistry* **33**, 1743–1752
6. Pearce, R.E., Rodrigues, A.D., Goldstein, J.A., and Parkinson, A. (1996) Identification of the human P450 enzymes involved in lansoprazole metabolism. *J. Pharmacol. Exp. Ther.* **277**, 805–816
7. Ibeanu, G.C., Ghanayem, B.I., Linko, P., Li, L., Pederson, L.G., and Goldstein, J.A. (1996) Identification of residues 99, 220, and 221 of human cytochrome P450 2C19 as key determinants of omeprazole activity. *J. Biol. Chem.* **271**, 12496–12501
8. Matsunaga, T., Ohmori, S., Ishida, M., Sakamoto, Y., Nakasa, H., and Kitada, M. (2002) Molecular cloning of monkey CYP2C43 cDNA and expression in yeast. *Drug Metab. Pharmacokinet* **17**, 117–124
9. Mitsuda, M., Iwasaki, M., and Asahi, S. (2006) Cynomolgus monkey cytochrome P450 2C43: cDNA cloning, heterologous expression, purification and characterization. *J. Biochem. (Tokyo)* **139**, 865–872
10. Tsao, C.C., Wester, M.R., Ghanayem, B., Coulter, S.J., Chanas, B., Johnson, E.F., and Goldstein, J.A. (2001) Identification of human CYP2C19 residues that confer S-mephenytoin 4′-hydroxylation activity to CYP2C9. *Biochemistry* **40**, 1937–1944
11. Richardson, T.H., Jung, F., Griffin, K.J., Wester, M., Raucy, J.L., Kemper, B., Bornheim, L.M., Hassett, C., Omiecinski, C.J., and Johnson, E.F. (1995) A universal approach to the expression of human and rabbit cytochrome P450s of the 2C subfamily in Escherichia coli. *Arch. Biochem. Biophys.* **323**, 87–96
12. Yasukochi, Y. and Masters, B.S. (1976) Some properties of a detergent-solubilized NADPH-cytochrome c(cytochrome P-450) reductase purified by biospecific affinity chromatography. *J. Biol. Chem.* **251**, 5337–5344
13. Omura, T. and Sato, R. (1964) The carbon monoxide-binding pigment of liver microsomes. I. Evidence for its hemoprotein nature. *J. Biol. Chem.* **239**, 2370–2378
14. Yamazaki, H. and Shimada, T. (1997) Progesterone and testosterone hydroxylation by cytochromes P450 2C19, 2C9, and 3A4 in human liver microsomes. *Arch. Biochem. Biophys.* **346**, 161–169
15. Tang, C., Shou, M., and Rodrigues, A.D. (2000) Substrate-dependent effect of acetonitrile on human liver microsomal cytochrome P450 2C9 (CYP2C9) activity. *Drug Metab. Dispos. Biol. Fate Chem.* **28**, 567–572

16. Gotoh, O. (1992) Substrate recognition sites in cytochrome P450 family 2 (CYP2) proteins inferred from comparative analyses of amino acid and coding nucleotide sequences. *J. Biol. Chem.* **267**, 83–90
17. Karam, W.G., Goldstein, J.A., Lasker, J.M., and Ghanayem, B.I. (1996) Human CYP2C19 is a major omeprazole 5-hydroxylase, as demonstrated with recombinant cytochrome P450 enzymes. *Drug Metab. Dispos. Biol. Fate Chem.* **24**, 1081–1087
18. Hofmann, T., Schwab, M., Treiber, G., and Klotz, U. (2006) Sensitive quantification of omeprazole and its metabolites in human plasma by liquid chromatography-mass spectrometry. *J. Chromatogr. B Biomed. Appl.* **831**, 85–90
19. Klose, T.S., Ibeanu, G.C., Ghanayem, B.I., Pedersen, L.G., Li, L., Hall, S.D., and Goldstein, J.A. (1998) Identification of residues 286 and 289 as critical for conferring substrate specificity of human CYP2C9 for diclofenac and ibuprofen. *Arch. Biochem. Biophys.* **357**, 240–248
20. Williams, P.A., Cosme, J., Ward, A., Angove, H.C., Matak Vinkovic, D., and Jhoti, H. (2003) Crystal structure of human cytochrome P450 2C9 with bound warfarin. *Nature* **424**, 464–468
21. Wester, M.R., Yano, J.K., Schoch, G.A., Yang, C., Griffin, K.J., Stout, C.D., and Johnson, E.F. (2004) The structure of human cytochrome P450 2C9 complexed with flurbiprofen at 2.0-A resolution. *J. Biol. Chem.* **279**, 35630–35637
22. Komori, M., Kikuchi, O., Sakuma, T., Funaki, J., Kitada, M., and Kamataki, T. (1992) Molecular cloning of monkey liver cytochrome P-450 cDNAs: similarity of the primary sequences to human cytochromes P-450. *Biochim. Biophys. Acta* **1171**, 141–146
23. Lewis, D.F., Watson, E., and Lake, B.G. (1998) Evolution of the cytochrome P450 superfamily: sequence alignments and pharmacogenetics. *Mutat. Res.* **410**, 245–270
24. Bridges, A., Gruenke, L., Chang, Y.T., Vakser, I.A., Loew, G., and Waskell, L. (1998) Identification of the binding site on cytochrome P450 2B4 for cytochrome b5 and cytochrome P450 reductase. *J. Biol. Chem.* **273**, 17036–17049
25. Morita, J., Kobayashi, K., Wanibuchi, A., Kimura, M., Irie, S., Ishizaki, T., and Chiba, K. (2004) A novel single nucleotide polymorphism (SNP) of the CYP2C19 gene in a Japanese subject with lowered capacity of mephobarbital 4′-hydroxylation. *Drug Metab. Pharmacokinet.* **19**, 236–238
26. Niwa, T., Kageyama, A., Kishimoto, K., Yabusaki, Y., Ishibashi, F., and Katagiri, M. (2002) Amino acid residues affecting the activities of human cytochrome P450 2C9 and 2C19. *Drug Metab. Dispos. Biol. Fate Chem.* **30**, 931–936
27. Jung, F., Griffin, K.J., Song, W., Richardson, T.H., Yang, M., and Johnson, E.F. (1998) Identification of amino acid substitutions that confer a high affinity for sulfaphenazole binding and a high catalytic efficiency for warfarin metabolism to P450 2C19. *Biochemistry* **37**, 16270–16279
28. Hasemann, C.A., Kurumbail, R.G., Boddupalli, S.S., Peterson, J.A., and Deisenhofer, J. (1995) Structure and function of cytochromes P450: a comparative analysis of three crystal structures. *Structure* **3**, 41–62
29. Graham-Lorence, S.E. and Peterson, J.A. (1996) Structural alignments of P450s and extrapolations to the unknown. *Methods Enzymol.* **272**, 315–326
30. Zhao, B., Guengerich, F.P., Bellamine, A., Lamb, D.C., Izumikawa, M., Lei, L., Podust, L.M., Sundaramoorthy, M., Kalaitzis, J.A., Reddy, L.M., Kelly, S.L., Moore, B.S., Stec, D., Voehler, M., Falck, J.R., Shimada, T., and Waterman, M.R. (2005) Binding of two flaviolin substrate molecules, oxidative coupling, and crystal structure of Streptomyces coelicolor A3(2) cytochrome P450 158A2. *J. Biol. Chem.* **280**, 11599–11607
31. Zheng, Y.M., Henne, K.R., Charmley, P., Kim, R.B., McCarver, D.G., Cabacungan, E.T., Hines, R.N., and Rettie, A.E. (2003) Genotyping and site-directed mutagenesis of a cytochrome P450 meander Pro-X-Arg motif critical to CYP4B1 catalysis. *Toxicol. Appl. Pharmacol.* **186**, 119–126
32. Kim, D. and Guengerich, F.P. (2004) Selection of human cytochrome P450 1A2 mutants with enhanced catalytic activity for heterocyclic amine N-hydroxylation. *Biochemistry* **43**, 981–988
33. Schoch, G.A., Yano, J.K., Wester, M.R., Griffin, K.J., Stout, C.D., and Johnson, E.F. (2004) Structure of human microsomal cytochrome P450 2C8. Evidence for a peripheral fatty acid binding site. *J. Biol. Chem.* **279**, 9497–9503
34. Williams, P.A., Cosme, J., Sridhar, V., Johnson, E.F., and McRee, D.E. (2000) Mammalian microsomal cytochrome P450 monooxygenase: structural adaptations for membrane binding and functional diversity. *Mol. Cell* **5**, 121–131
35. Scott, E.E., He, Y.A., Wester, M.R., White, M.A., Chin, C.C., Halpert, J.R., Johnson, E.F., and Stout, C.D. (2003) An open conformation of mammalian cytochrome P450 2B4 at 1.6-A resolution. *Proc. Natl Acad. Sci. USA* **100**, 13196–13201